Desalination and Water Treatment
www.deswater.com

doi: 10.5004/dwt.2020.25894

195 (2020) 64–78
August

Seawater desalination through natural temperature difference: an experimental, theoretical, and place case study

Mona Shojaei[a], Mohsen Nosrati[b,*], Reza Attarnejad[c], Bahram Saghafian[d]

[a]*Technical and Engineering Department, Science and Research Branch, Islamic Azad University Tehran, Iran, Tel. (+98) 21-4486-8540; email: shojaei.mon@gmail.com (M. Shojaei)*
[b]*Biotechnology Group, Chemical Engineering Department, Tarbiat Modares University, P.O. Box: 14115-143, Tehran, Iran, Tel. (+98) 21-8288-4372; email: mnosrati20@modares.ac.ir (M. Nosrati)*
[c]*School of Civil Engineering, College of Engineering, University of Tehran, Tehran, Iran, Tel. (+98) 21-6111-2225; email: attarnjd@ut.ac.ir (R. Attarnejad)*
[d]*Technical and Engineering Department, Science and Research Branch, Islamic Azad University Tehran, Iran, Tel. (+98) 21-4486-8540; email: b.saghafian@gmail.com (B. Saghafian)*

Received 29 July 2019; Accepted 24 March 2020

ABSTRACT

Sub-atmospheric vapor pipeline (SAVP) transfer is a new trend for water desalination that transports vapor from a warm area to a cold area, with many benefits. The theory, experiments, and field calculations of SAVP transfer for seawater desalination have been studied. The theory of this study has been based on the transmission line and mass and energy balance of a compressible fluid. In the laboratory section, equipped with a heating and an evaporating system for saline water (three salinities levels), a transmission line (three diameters) with different temperatures of the warm and the cold sources were employed on vapor transfer experiments. In the field section, vapor transmission with 1, 2, and 4 m diameters were studied with respect to the city of Bandar Abbas and Geno elevations at a distance of 30 km. It was determined that diameter, temperature difference, and salinity were the three factors affecting the efficiency of the SAVP transfer, respectively. The results of this study were presented in the mass outlet flow of condensed water at the destination. Given the margins of confidence and technical guaranty in calculations and implementation, it has been scientifically proven that the results of this study were significantly higher than previous studies.

Keywords: Seawater desalination; Vapor pipeline; Natural temperature difference; Sub-atmospheric vapor pipe line (SAVP); Compressible flow

1. Introduction

The evaporation of seawater in warm regions, its transmission with clouds, and finally its condensation as rain in low temperatures is a clear example of the natural desalination of seawater, which annually provides billions of tons of desalinated water for various parts of the world. The basis of such natural desalination is the meaningful difference between the warm source (sea) and the condensation location, which has become the purpose of studies for some researchers to investigate desalination through natural potentials [1,2]. Among the requirements for this method which is called "sub-atmospheric vapor pipeline (SAVP)," there is the existence of a cold area that provides a sufficient temperature difference for the transmission and the condensation of vapor which is performed by a natural or an artificial condenser. From a climatologically point of view, the SAVP method is efficient when vapor transmission through a sub-atmospheric pressure drop from seawater to cold heights adjacent to the sea takes place. By the help of ambient (sea) warm temperature, water vapor emits out from the salty water trough evaporation and travels toward a cold ambient (mountain)

* Corresponding author.

via an insulated pipe. After transmission, the vapor is condensed and a sort of desalinated water is generated on the top of the cold ambient. Evaporation causes vacuum due to the extreme volume reduction of the fluid followed by pressure drop. The level of the pressure drop depends mainly on the difference between temperatures in the warm source (sea level) and cold source (mountain); the more temperature difference, the more vapor flow rate. Coastal cold and dry mountains near to the free oceans are the best places suitable for SAVP. Once the system wants to be started, it would be commissioned under an initial vacuum. Vacuum is done only once; then the condensation itself causes a pressure drop for fluid movement permanently.

Like Al-Quran (in the Hashemite Kingdom of Jordan) and Sana'a (the capital of the Republic of Yemen) where have higher elevation and lower temperature in comparison to free sea level and temperature, many of the cities and regions located in the Middle East have the same conditions that make water provision through the SAVP method possible and attractive.

Using the natural potentials mentioned above, seawater desalination and transfer in such hot and dry areas are found extremely attractive and justifiable. Although, the low rate of desalinated water transfer and the need to find natural hot and cold sources are the limitations of the SAVP transfer method, numerous advantages, and strong points can be associated with this method from industrial and economical points of view. From the viewpoint of energy-consumption reduction or even elimination, the benefits such as elimination of the heat source or condenser (and their associated materials and equipment), extreme reduction in energy consumption related to water transfer, the possibility of regaining energy at the transfer destination by using a water turbine, water distribution by gravity, and the use of advantages allocated by the Paris Convention (February 2006) for decrease carbon dioxide emission, have made desalination through SAVP to a highly preferable method among other methods [3].

Although new low-cost and low-energy consumption researches (based on new techniques or sources) are being developed [4,5], the basic knowledge about desalination says that the current desalination methods, nowadays, are reverse osmosis (RO), multi-effect distillation/multi-effect distillation-thermal vapor compression (MED/MED-TVC), and multi-stage flash (MSF) which produce a huge amount of desalinated water especially in the middle east [6–8]. From the viewpoint of applicability and full-scale production, these methods (especially distillation methods) are very common, reliable, and trustworthy [9]. According to a very new industrial reference published by the International Water Summit (IWS on 2018 January), RO consumes 4.0–4.5 kWh; whereas, MED and MSF consume 16.0–18.5 and 22.5–25.0 kWh for 1 cm^3 desalinated water, respectively. These energies are called equivalent electrical energies [10]. For water transmission by pumping, depended on the distance and elevation, more electrical energy must be consumed. Although SAVP could be a useful method for water supply, it is a different desalination method that could be applied in a certain area (mentioned above), therefore, it should not be compared to common methods (RO, MED, and MSF) individually or in single directions, for example, the quantity, energy consumption, technology, vastness, and etc.

Numerous studies on seawater desalination through only temperature differences for evaporation and condensation are available in the form of journal articles [11–17]. In addition, those technical and industrial studies related to applied researches have been published in the patents [2,18–25]. Also in recent years, some more publications have been published [26–28]. In all of these studies, an element called "transmission line" does not exist essentially. Therefore, desalination takes place locally (not via a long pipeline).

This research, experimentally and theoretically, has studied the SAVP transmission issue over long distances through an adequate formulation for the determination of mass and momentum transfer in an evaporation and condensation sections. For better expression on scientific and experimental contributions, the present study used a large and detailed set-up with more thermal and cooling details along with vapor transmission pipes having various diameters. Meanwhile, creation of realistic and compatible climatic conditions for the origin and the destination, removal of the limitation on the length of condensation (L_C), an estimate of the exact saltwater evaporation by using the thermodynamic function Φ (osmotic coefficient), sufficient repeat, and proper timing for stabilizing the vapor transmission data and proof of its repeatability, tests through creating different salinities, and finally, considering of vapor compressibility are the technical contributions of this study that can lead to the advancement of knowledge and technology in the SAVP transmission method. In order to extend experimental knowledge to real field studies, the coastal city of Bandar Abbas (situated in the south of Iran), as a city with specific features of a warm source and Geno heights (2,300 m) 30 km away (to the northwest of Bandar Abbas) of cold source have been selected for inland studies.

2. Materials and methods

2.1. Theory

In short tubes and nozzles, one can ignore the effects of viscosity especially for transmission of gasses. However, in long tubes (conditions that are consistent with the nature of this study), the effects of flow friction on the wall of the pipe must be considered. In order to provide a practical formulation, considering the friction, a limited volume of a pipe is considered, and by the balance of mass and momentum, the equations governing the fluid transfer will be derived. Finally, the result of the formulation for the total length of transfer is presented. The physical recognition of the problem and the understanding of the nature governing the vapor transmission, including the linear distance, and the height between the cold and the warm points, and the range of temperature variations between these points are considered as the most important primary knowledge of the issue.

The pipeline can be composed of a large number of interconnected tubes (segments), the thermodynamic conditions at the beginning and at the end of each tube are different, and each segment has its own specific fluid velocity. The initial estimation for the velocity in the first element alongside the use of ideal gas equation and the Antoine equation (for the relationship between saturated vapor pressure and its temperature) eliminate the unknown variables that only

one unknown variable (including the pressure (P) or density (ρ)) has remained for the end of the element which is easily solvable. The assumption of being saturated for vapor in the entire transmission path (and in all the elements), causes the remaining unknowns such as the temperature to be solved at the end of each element. This trend will be repeated for other elements up to the end of the transmission line, which will result in the determination of the temperature at the end of the transmission line too. The comparison of the calculated temperature with the natural cold source temperature (along with the calculation of the total pressure drop) will cause the calculation of the final element to be repeated until the two temperatures are closely aligned with accuracy. This attitude, while adhering to the principle of the compressibility of vapor, can provide accurate calculations of velocity, density, and pressure variations in the path.

2.2. Mass and momentum balance in flow transfer

Fig. 1 depicts an inclined pipeline (α degree) with a constant diameter as an example of a transmission pipeline for the SAVP method, in which mass and momentum balance can be generally shown with Eqs. (1)–(3). Eq. (2) could be read as a simplified form of the global Navier–Stokes equation in Cartesian coordination and single direction path. The transfer generally takes place from point 1 and continues to point 2. Pressure, density, velocity, and fluid height are shown with the symbols P, ρ, U, and H, respectively.

$$\frac{\partial \rho}{\partial t}+\frac{\partial(\rho U)}{\partial x}=0 \tag{1}$$

$$-\frac{\partial(\rho U^2)}{\partial x}-\frac{\partial P}{\partial x}-\frac{4}{D}\tau_w-\rho g.\sin(\alpha)=\frac{\partial(\rho U)}{\partial t} \tag{2}$$

where ρ, U, P, D, τ_W, g, and α represent vapor density, vapor velocity, vapor pressure, pipe diameter, wall shear stress, gravitational acceleration, and the angle of pipeline relative to the horizon, respectively. By using the definition of the Fanning friction factor, f in the Eq. (3a), τ_W can be omitted from Eq. (2). Therefore:

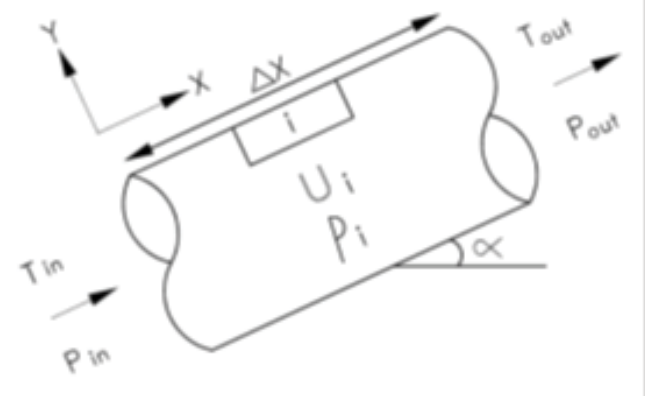

Fig. 1. Schematic diagram for an element of SAVP transmission.

$$\tau_w=\frac{1}{2}f\rho U^2 \tag{3a}$$

$$\frac{\partial(\rho U)}{\partial t}+\frac{\partial}{\partial x}\left(\rho U^2+P\right)+\rho g.\sin(\alpha)+\frac{2f\rho U^2}{D}=0 \tag{3b}$$

$$\frac{1}{\sqrt{f}}=-4\log\left(\frac{\frac{\varepsilon}{D}}{3.7}+\frac{5.74}{\text{Reynolds}^{0.9}}\right);5{,}000<\text{Re}<10^8 \tag{3c}$$

The friction factor (f) could be determined by the empirical relation [29] given by Eq. (3c) (for smooth pipes ϵ/D will be omitted). Simultaneously, solving Eqs. (1) and (3b), variations of density, velocity, and pressure along the transmission pipe can be calculated. Solving Eq. (3b) is an example of simulating the problem in an unsteady state. In this simulation, variations of the variables are considered with time. Moreover, the accumulation of vapor in the pipe is taken into account.

Eq. (3b) can be significantly simplified based on the user's assumptions. Under steady-state conditions, the first term of both Eqs. (1) and (3b) will be omitted. Meanwhile, assuming the fluid to be incompressible, density will be assumed constant along the path, and will exit the differential. In the steady and incompressible simulation, a variation of variables with time and the amount of vapor accumulation in the pipeline will not be considered. In the field and operational studies, once the average temperatures for each month of the year are considered and recorded in 12 figures (across the year) entering calculations, a steady condition was actually assumed to solve Eq. (3b), which is not far from reality. Owing to search and climate studies (especially temperature) that are focused on monthly reports, collecting, analyzing, and using the average monthly variables (from January to December) are inevitable. Therefore, whether or not, when studying and modeling, changing of variables with time ($\partial\rho/\partial t$), will be omitted. In this study, in order to solve an analytic problem, the assumption of steady-state and compressibility of the fluid (that is as close as possible to reality), will be considered as the basis of the calculations. Considering the pipe length to be L, and the slope of the transmission line to be α, Eq. (4a) will be obtained which contains three pressure drops including compressible pressure drop (ΔP_ρ), hydrostatic pressure drop (ΔP_H), and friction pressure drop (ΔP_f).

$$-\Delta P=\Delta\rho\cdot U^2+\rho gL\cdot\sin(\alpha)+\frac{2fL\rho U^2}{D} \tag{4a}$$

$$\Delta P_\rho=\Delta\rho\cdot U^2 \tag{4b}$$

$$\Delta P_H=\rho gL\cdot\sin(\alpha) \tag{4c}$$

$$\Delta P_f=\frac{2fL\rho U^2}{D} \tag{4d}$$

The element computational algorithm for this study is presented in Fig. 2. The small lengths for the tubes will slow down the calculations and be disregarded for the final answers. On the other hand, if these lengths are large, although increases the speed of computations, the accuracy of the outputs will be greatly reduced.

Hence, after obtaining the experience in the numerical solution of Eq. (4a), taking a length of 1,000 m will result in an increased speed of the numerical calculations and obtains the desired accuracy. If the incompressible fluid is considered, the first term of the right side of Eq. (4a) will be omitted. The steady-state conditions and incompressibility (for small

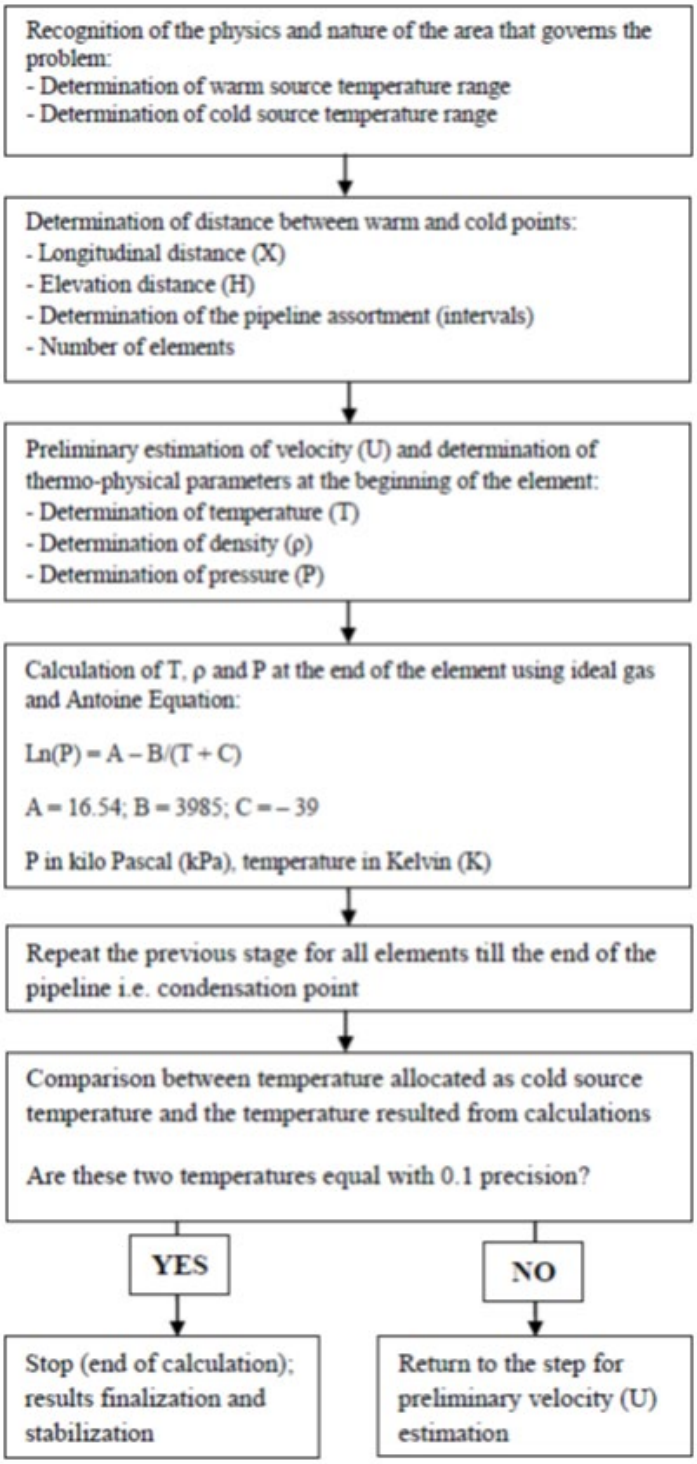

Fig. 2. Flow chart of the pipeline iterative calculation.

segments) will only remain two terms of the pressure drop, $\rho g L \cdot \sin(\alpha)$ and $2fL\rho U^2/D$, which will include the unknown velocity U. The designation of this study is the velocity determination with the assumption of the compressibility (for entire pipe) to estimating the parameters iteratively until achieve proper answer. While we calculate all unknowns by the method presented in the algorithm introduced in Fig. 2, other investigators [1] tried to determine the velocity by the following empirical relation for incompressible fluid [30], with an important limitation for Re number ($3 \times 10^3 < \mathrm{Re} < 10^5$):

$$U = \left(\frac{2\Delta P_f}{0.3164 L}\right)^{\frac{4}{7}} \left(\frac{D^5}{\rho^3 \mu}\right)^{\frac{1}{7}} \tag{5}$$

3. Experiments

3.1. SAVP experiments

3.1.1. General description of the SAVP experimental setup

A laboratory set-up was designed and conducted for the experimental study of SAVP desalination and vapor transmissions in a hydraulics lab (room temperature 20°C). This set-up has been schematically shown in Fig. 3. The sizes and the dimensions shown in this figure are not representative of actual sizes and dimensions, and have been only shown for a technical understanding of the system and how it works. This system is composed of three main components, that is, evaporator (A), transmission pipe (B), and condenser (C).

A long copper transmission pipe, insulated with an elastomer (1), connects the evaporator to the condenser. The transmission pipe could have different diameters (i.e., ½, ¾, and 1 inch). The pipe has 180 m long, however, it was rounded and twisted around a vertical column having a height of 11 m (the pipe coil has not been shown). A vacuum pump (2) helps to have an initial vacuum in pipeline and condenser; this vacuum pump is used only for a startup (for only one-time use). The SAVP consists of enough valves and fittings for stabilization and vibration problem shooting. For each test (or startup), the salinity of the saline water, evaporator temperature, and condenser temperature were adjusted. Initially, there was nothing existing but the air inside the pipe and condenser. This air was vacuumed by the vacuum pump. Once air exiting process was completed, the vacuum pump was turned off (no more vacuum). By opening the inlet valve of the pipe very gradually, the liquid in the evaporator evaporates. The inlet valve to the condenser now could be opened. Once vapor condensed in the condenser, the condensate is accumulated in a 10 m collecting column (3) without vacuum break. Due to the condensation in the condenser, a natural volume reduction and consequently pressure drop will be generated that causes more vapor to be transferred and reaches to the condenser. In this way, the SAVP works continuously. Data were collected after assuring the system is in steady-state condition.

3.1.2. Setup specifications

The volume of the evaporator is big enough (actual 120 L) so that evaporation will not cause a significant change on degree of salinity during the tests. The provision of cold air with an appropriate blow for the condenser was very difficult to come by in the laboratory. Therefore, an air conditioner (4), with an outlet air temperature of about 0°C, and a blower (5), equipped with a heater, was used. This blower can provide a desirable temperature for contact with the condenser through interference with the cold stream of the air conditioner. An agitator (6) alongside an electric heater (7) and baffles (8), which divides the evaporator tank into three parts, form the evaporator assembly. The energy required for

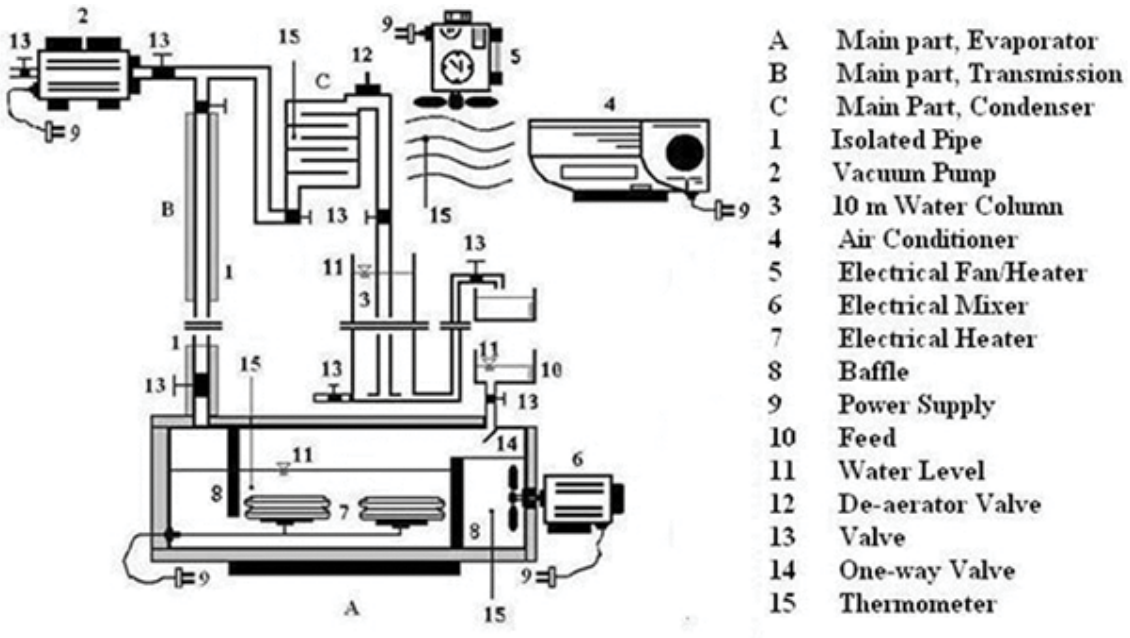

Fig. 3. View of the desalination laboratory setup.

the vacuum pump, blower, and electric heater is supplied by the city's electric power (9). A local feed intake (10) has also been contemplated. The water levels (11) in the evaporator, the water collecting column, and the feed tank can be fixed or adjusted for use. Three types of valves, including the air valve (12), on–off valve (13), and non-return valve feed (14) have been used in this desalination set. Alcohol thermometers or temperature sensors have been installed (15) at key locations. Table 1 lists the quantitative values of the desalination setup components.

3.2. Commissioning and operation

This desalination system works based on the natural phenomenon of vapor production in the warm source (sea level) and its condensation in a cold environment (mountain heights). The designed system is capable of preparing water with different salinities in terms of initial density distribution and heat (T_s; warm source temperature). Salinity is adjusted through feeding saturated saline water in a small tank above the evaporator and the agitator inside. The provided baffles make it possible to adjust the density of the vapor and prevent it from exiting before the fluid becomes homogeneous in terms of mass and heat.

The vacuum pump can empty all or a part of the path from the air (if necessary). Water is heated in the insulated evaporator tank with adjusted salinity and temperature and reaches to mass and thermal equilibrium. When the connecting valves between the evaporator and the condenser are slowly opened, vapor occupies the entire path, and condensation occurs in the condenser with the help of cold air flow from the air conditioner. Since every condensation comes with a significant reduction in fluid volume, the desalination system (without vacuum pump intervention) is continuously performed. In case of vacuum failure due to operation error or any other reasons, the vacuum pump can be turned on/off if necessary.

4. Thermo-physical properties and calculations

The thermo-physical properties of seawater include density, viscosity, evaporation latent heat, boiling point, and osmotic seawater pressure; empirical data and good mathematical relations are available [31]. The thermodynamics of electrolyte solutions with variations in mean ionic activity coefficient ($\pm\gamma$) of salt and osmotic coefficient (Φ) of water were also measured already [32]. According to Eq. (6), water activity (a_w) is associated with the osmotic coefficient of

Table 1
Quantitative values of desalination setup components

No.	Description	Capacities (cap.) and remarks
A	Evaporator	Total volume 150 L
		Actual volume 120 L
		Insulated, cast iron, vacuum sealed
B	Transmission line	180 m length
		11 m height (skein and rounded)
		Copper, standard insulation
		1/2, 3/4, and 1 inches diameter (0.01270, 0.01905, 0.02540 m)
C	Condenser	Around 2 L, spare part of the air conditioner
1	Isolated pipe	Elastomer standard insulation
2	Vacuum pump	Edwards RV5; England; cap. 4.1 ft^3/min (0.1161 m^3/min)
3	10 m water column	10 m length
		Copper; 1/2 inch diameter (0.01270 m)
4	Air conditioner	Cap. 800 m^3/h, air moisture removal 2.7 L/h
		4,800 W; 1/2 inch; core temperature –20°C; outlet temperature around 0°C
		(1 inch is equal to 0.0254 m)
5	Electrical fan/heater	Maximum temperature 70°C, Maximum 300 m^3/h
6	Electrical mixer	Power 0.2–4.0 kW; maximum rpm 1,720; 50 Hz
7	Electrical heater	2 × 4.0 kW (maximum), adjustable
8	Baffle	Plastic baffles
9	Power supply	220 V, 50 Hz
10	Feed	Feed zone, salty water, and salt
11	Water level	Indicator
12	De-aerator valve	For de-aeration
13	Valve	Valves used in a air conditioner
14	One-way valve	One direction valve
15	Thermometer	Bulb and transmitter

saline water. On the other hand, the thermodynamic activity of water, which is the key to the equilibrium calculation of water evaporation and condensation, is related to the ratio of saline water vapor pressure and pure water vapor pressure. This relation is expressed in Eq. (7).

$$\Phi = \frac{-55.1}{2m} \cdot \ln a_W \tag{6}$$

$$a_W = \frac{P_{sw}^{sat}}{P_{pw}^{sat}} \tag{7}$$

Where, P_{sw}^{sat} is the saturation pressure of saline water or seawater, and P_{sw}^{sat} is the saturation pressure of pure water. Therefore, salinity will have a direct effect on the liquid-vapor pressure and the degree of evaporation. The amount of salinity (S) in terms of molality (mo) is inversely proportional to the ease of desalinating.

5. Field properties

When SAVP is supposed to be applied in the natural field, the magnitude of the difference between the cold and warm source temperatures as well as distance between these two sources are very important parameters from the viewpoint of plant feasibility. More temperature differences and less distances result in more vapor transmission. If these two priorities are met, the only technical and operational concern would be the height difference between the two temperature sources. In any case, the mentioned items can have efficient results.

A case study with satisfying results was observed in the desalinated water transfer through SAVP method from the coastal city of Bandar Abbas (south of Iran) to the cold 2,300 m high Geno region (north-west Iran) located around 30 km away. Meteorological data related to sea-level temperature in Bandar Abbas (the warm source) and the Geno heights (the cold source) have been depicted in Fig. 4; each temperature that is shown with a point is the average of the recorded temperatures during 1 month. In Geno heights, the average daily (maximum) and nightly (minimum) temperatures were reported each month, whereas for Bandar Abbas, owing to the negligible difference between day and night temperatures at sea level, only 1 monthly average temperature was reported [33].

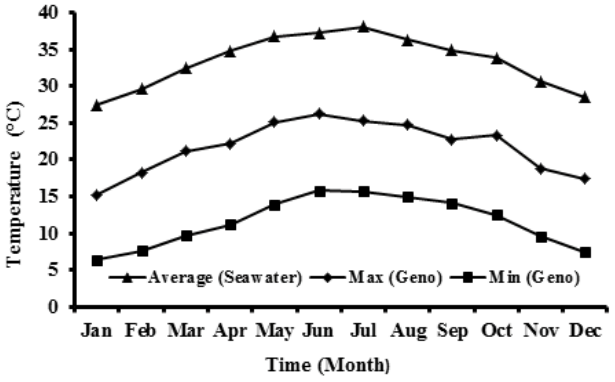

Fig. 4. Geno mount and Bandar Abbas sea level temperature during 1 y.

6. Results and discussion

6.1. Laboratory system

The vapor transmitting pipe diameter, the temperature difference between the origin and the destination, and salinity were the three most important and influential parameters in calculating the efficiency of desalination via SAVP. Based on the sequence of tests mentioned in the section Materials and methods, desalinated water production was tested for various pipe diameters (1/2, 3/4, and 1 inch), temperature differences (25°C, 20°C, 15°C, and 10°C), and water salinity (0.2, 1.5, and 4.0 wt.%), and the results were presented in Table 2.

Experiments based on different pipe diameters were conducted to determine the effect of pipe size on the amount of transferred vapor mass. The four temperature differences, logically, and experimentally, include all the temperature differences that can occur during the summer and the winter between the warm source (sea-level) and the cold source (mountain). From the viewpoint of phase equilibrium thermodynamics and despite of seawater desalination, the SAVP transfer desalination method, can be used for low salinity fluids such as low-salinity brackish waters and wastewaters. Consequently, the completion of laboratory studies and modeling requires that these sources of waters are also experimented for SAVP desalination. In this respect, salinities of 0.2 and 1.5 wt.% (despite of 4.0 wt.% for seawater) were also tested for typical wastewaters and low-salinity brackish waters, respectively.

To find the controversial results that proved the performance of the model and the device, no experimental design was performed and all the experiments were carried out in accordance with the full factorial approach. The system's operating time for all tests was measured right after the system was warmed up and immediately after opening valve 13 (located on pipe B) and the produced freshwater weight was measured. These experiments were repeated three times and their average amount was determined. To compare the data, they were all reported in grams per day.

Based on these variables (diameter, temperature difference, and salinity), a 21-times difference can be observed in desalinated water production from a minimum of 222 to a maximum of 4,695 g/d. Focusing on Table 2, it can be observed that the diameter change is the most influential parameter in desalinated water production (which can be expected).

As the pipe diameter increases, SAVP transmission also increases. The other two parameters, the temperature difference between origin and destination, and seawater salinity, are the next most important factors. Salinity is more important in smaller diameters.

The tests mentioned in Table 2 can be simulated based on the general theory of fluid transmission in the steady-state condition by using Eq. (4). The calculated values (cal), which are based on the system becoming steady and free from warming up, primary fluctuations, and incompressibility, have been mentioned in the same table after the experimental

Table 2
Effect of pipe diameter, temperature difference, and water salinity on experimental desalinated water production through SAVP

	D = 1/2 (inch)						D = 3/4 (inch)						D = 1 (inch)					
T_S	25			30			25			30			25			30		
T_C	5	10	15	5	10	15	5	10	15	5	10	15	5	10	15	5	10	15
	RMSD = $\sqrt{\frac{1}{n}\sum_{i=1}^{n} \lvert m_{exp} - m_{cal} \rvert^2}$ = 121 (g/ d)																	
	Salinity (S) = 0.2 wt%																	
m (g/d)	740/751/(1.46%)	500/508/(1.57%)	390/396/(1.51%)	1,070/1,085/(1.38%)	743/754/(1.45%)	529/538/(1.67%)	2,630/2,580/(–1.93%)	2,114/2,050/(–3.12%)	1,872/1,798/(–4.11%)	2,900/2,810/(–3.20%)	2,690/2,598/(–3.54%)	2,231/2,127/(–4.88%)	4,296/4,115/(–4.39%)	3,963/3,774/(–5.0%)	3,690/3,498/(–5.48%)	4,695/4,500/(–4.33%)	4,343/4,145/(–4.77%)	4,059/3,855/(–5.29%)
	RMSD = $\sqrt{\frac{1}{n}\sum_{i=1}^{n} \lvert m_{exp} - m_{cal} \rvert^2}$ = 117 (g/ d)																	
	Salinity (S) = 1.5 wt.%																	
m (g/d)	670/675/(0.74%)	456/457/(0.21%)	314/318/(1.25%)	979/981/(0.2%)	651/657/(0.91%)	459/465/(1.29%)	2,500/2,430/(–2.88%)	1,992/1,941/(–2.62%)	1,758/1,722/(–2.09%)	2,812/2,716/(–3.53%)	2,546/2,471/(–3.03%)	2,090/2,030/(–2.95%)	4,176/3,972/(–5.13%)	3,840/3,660/(–4.91%)	3,574/3,401/(–5.08%)	4,538/4,329/(–4.82%)	4,222/4,032/(–4.71%)	3,950/3,760/(–5.05%)
	RMSD = $\sqrt{\frac{1}{n}\sum_{i=1}^{n} \lvert m_{exp} - m_{cal} \rvert^2}$ = 103 (g/ d)																	
	Salinity (S) = 4.0 wt.%																	
m (g/d)	533/537/(0.74%)	363/368/(1.35%)	222/225/(1.33%)	845/855/(1.16%)	561/567/(1.05%)	345/347/(0.57%)	2,304/2,240/(–2.85%)	1,751/1,697/(–3.18%)	1,584/1,540/(–2.85%)	2,610/2,530/(–3.16%)	2,300/2,240/(–2.67%)	1,804/1,750/(–3.08%)	3,940/3,800/(–3.68%)	3,623/3,450/(–5.01%)	3,358/3,170/(–5.93%)	4,273/4,100/(–4.21%)	4,056/3,901/(–3.97%)	3,678/3,502/(–5.02%)

T is in °C degrees and m is in grams per day (g/d).
Vertical numbers from top to bottom indicate the laboratory values, theoretical values, and the RMSD.
One inch is equal to 2.54 cm or 0.0254 m.

numbers (exp); so that they can be compared with each other. In Eq. (4), there is no salinity, but the thermodynamic empirical data [31], alongside Eqs. (6) and (7), can theoretically provide a precise estimate of vapor pressure and, consequently, the mass of the vapor and the amount of condensed water. Moreover, point-to-point error has been presented in each cell and the total error has been calculated based on the root-mean-standard deviation (RMSD) and shown beneath each test.

Pressure that moves the fluid inside the tube and decreases according to the rules governing fluid mechanics, is the vapor pressure of salty water and must be calculated and corrected with Eqs. (6) and (7). The effect of these two equations on the results of calculations of freshwater production in the laboratory and the field scale are considered. The thermodynamic behavior of the sodium chloride solution in the form of an osmotic coefficient (Φ) is an interesting behavior [32]. At salt concentration equal to zero, the osmotic coefficient is equal to 1, showing the solution is in its thermodynamically ideal condition and the water activity coefficient (γ_W) is equal to one too. However, as the salt concentration increases in the solution, the osmotic coefficient decreases significantly and this decreasing behavior continues until it reaches a minimum (0.92) at salt concentration about 0.4 molals. Once again, with increasing salt concentration, the osmotic coefficient also approaches and even crosses the unity (1.00) again at near 2.4 molals. This behavior can justify the production of freshwater from concentrated brines in other desalination systems.

It is obvious that the outputs from a model will be reliable when they are as close as possible to the experimented values. Moreover, for scale-up and any applied or industrial approaches, determined numbers are trustable when they appear less than experimented ones but closed to them. This principle can be observed in Table 2. An error of approximately 3% and 5% are calculated for 3/4 and 1 inch diameters, respectively, which are both less than the experimental values in all the salinities. For a 1/2 inch diameter, the experimental values are higher than calculated values, this does not, however, damage the authenticity of the model, as the point error in this part of the test is only about 1%. As the diameter is increased, the compressible behavior of the fluid occurs gradually and is then intensified. The increase in RMSD in larger diameters can be attributed to this fact. In all states that were categorized as 0.2, 1.5, and 4.0 wt.% of salinity, RMSD did not surplus 121 g/d. The average of this deviation was 114 for the three sets of tests based on salinity.

A visible and analyzable figure that can explain the trend of water production is given in Fig. 5. This Fig. 5 demonstrates the effect of pipe diameter, temperature difference, and raw water salinity. Water production was determined and illustrated in *y*-axis and temperature difference, as an independent variable, was given in the *x*-axis. Also, pipe diameter and salinity were given as two other independent variables. Fig. 5 was arranged in a way that the importance of the variables and their influence on water production could be able to be seen and analyzed by reader. Temperature differences from 10°C to 25°C and diameter variation from 1/2 to 1 inch caused a water production from 225 to 4,500 g/d (20 folds). Fig. 5 shows that the diameter change is the most influential in desalinated water production. Despite of the pipe diameter that seems to be the most significant factor, the salinity has less effect on water production. Although, compared to pipe diameter, salinity showed to have less effect, it demonstrated around 30% in water production for small diameters when it changed from 0.2 to 4 wt.%. In other words, the effect of salinity could be more significant and sensible in pipes having small cross-section area.

The condenser's condensation power is selected through the installation of the air conditioner in such a way that it is possible to condense the inlet cold vapor even in the highest transmission flow. Therefore, there is no need for consideration and calculation of the condensation length in this study. The philosophy behind the installation of a condenser involves omitting the limitation of desalinated water production related to the length of the condenser (L_C) at the destination, which results in the elimination of calculations and tests related to wind-blow. In this way, comprehensive studies can be performed on salinity and the diameter effect. In these tests, the temperature difference between the origin and the destination has not been for complicating the condenser section, but rather for creating a driving force as the main cause of motion. In the large-scale design, the calculation of condensation length (L_C) and its estimation for complete condensation is necessary due to the fact that a compact condenser system, such as a thermal transformer, will not be designed and installed after the transmission section.

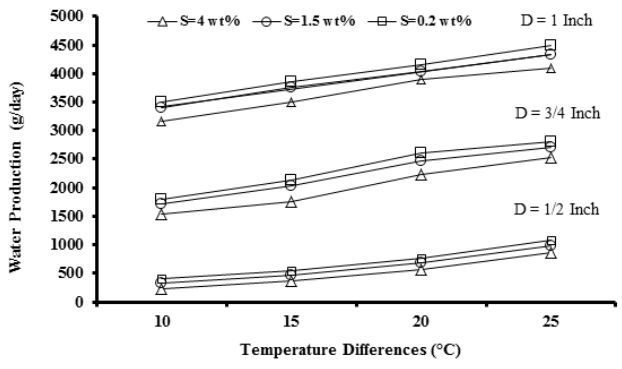

Fig. 5. Trend of the pipe diameter, temperature difference, and water salinity on experimental desalinated water production.

6.2. Model calculations for actual inland dimensions

The average origin warm temperature for seawater in the Bandar Abbas coast, and the maximum and minimum temperatures for Geno heights have been illustrated in Fig. 4. Calculations related to Eq. (4) will result in a steady calculation for each month, which has been reported for 1, 2, and 4 m diameters in Table 3. For each month, the average seawater temperature (warm source), and the average minimum and maximum temperature for the cold source are shown in Fig. 4. This difference in temperatures produces mass (*m*, kg/s) of desalinated water, as indicated in Table 3. As expected, in the months when the average temperature difference between the source of warm and cold is higher, the vapor condensation is also expected to increase, followed by increasing in desalinated water production. In all cases,

Table 3
Vapor transmission calculations based on SAVP for diameters of 1, 2, and 4 m for Bandar Abbas to Geno along with results of calculations based on Inoue et al. [1]

Month	D = 1 m				D = 2 m				D = 4 m			
	[1] (cal.)	This work (cal.)		This work (cal.)	[1] (cal.)	This work (cal.)		This work (cal.)	[1] (cal.)	This work (cal.)		This work (cal.)
	m (kg/s)	m (kg/s)	Diff. (%)	Re × 10^3	m (kg/s)	m (kg/s)	Diff. (%)	Re × 10^3	m (kg/s)	m (kg/s)	Diff. (%)	Re × 10^3
January	0.132	0.203	34.9	11.588	1.614	1.824	11.5	104.118	6.451	7.941	18.7	453.291
Febuary	0.148	0.232	36.2	13.243	1.693	1.916	11.6	109.37	8.204	9.94	17.4	567.398
March	0.164	0.284	42.2	16.211	1.752	2.16	18.8	123.298	9.558	12.314	22.4	702.912
April	0.274	0.346	20.8	19.75	1.887	2.312	18.3	131.974	10.627	13.259	19.8	756.854
May	0.289	0.391	26.1	22.319	1.975	2.43	18.7	138.71	12.38	14.978	17.3	854.979
June	0.294	0.396	25.7	22.605	2.141	2.482	13.7	141.678	12.233	14.823	17.4	846.131
July	0.372	0.434	14.3	24.774	2.083	2.396	13.1	136.769	12.634	15.101	16.3	862
August	0.307	0.371	17.2	21.178	2.011	2.294	12.3	130.947	11.951	14.244	16.1	813.08
September	0.259	0.337	23.1	19.237	1.716	1.923	10.7	109.769	9.484	12.138	21.8	692.865
October	0.287	0.368	22.1	21.006	1.729	2.04	15.2	116.448	10.336	12.561	17.7	717.011
November	0.202	0.269	24.9	15.355	1.66	1.876	11.5	107.086	8.101	9.84	17.6	561.69
December	0.186	0.218	14.6	12.444	1.631	1.811	9.9	103.376	7.404	8.137	9.1	464.479

Diff. means difference between two formulations and “cal.” stands for “calculated”.

during the summer period, including May, June, and July, the highest condensation rate has occurred.

If the formulation of a similar work [1] is run for Bandar Abbas/Geno field, we will encounter to the numbers that are marked in Table 3. Although this reference studied vapor transmission for two coastal areas, that is, Al-Quren (Jordan) and San'a (Yemen) via an acceptable approach to material balance between three sections of evaporation, transmission, and condensation, it does not include complimentary preconditions reviewed in the last paragraph read in the "Introduction" section of the present work. In all cases, the numbers of our calculation are more than numbers calculated by them. Although their results provide certainty, they appear to have been exaggerated in the direction of lower mass calculation for desalinated water. Owing to stepwise calculations of numerous elements (related to SAVP transmission), the application of the compressible conditions and the application of the Antoine's equation, the results of our research are more systematic and more scientific, even with the consideration of the effect of salinity (which reduces evaporation), the numerical results of our research are greater in all respects.

Fig. 6 represents the relationship between velocity, density, and temperature for SAVP via three different diameters, that is, 1, 2, and 4 m. More diameters cause more flow followed by more vapor velocity. By increasing the diameter, flow, and velocity (U) increase drastically. The ground path between Bandar Abbas and Geno, spanning around 30 km, is divided into 30 length elements of 1,000 m, each of which has its own vapor velocity (left vertical axis). Owing to the expansion of the fluid in the transmission line and the receipt of compressibility conditions, the vapor density clearly decreases. The vapor density drop (4 m diameter pipeline, 45–19 g/m^3) is considered to be more than 50% in this transfer indicates that the transmission is occurred under compressible condition. Reducing the temperature (4 m diameter pipeline, 37°C–23°C) and reducing the water vapor density is visible from the right vertical axis both for 4 m diameter pipeline.

From the laboratory point of view and in proportion to the diameter, the results of the mass flow of our study, even with regard to salinity, are greater. A diameter of about 0.35 inches can cause certain wall effect due to increase the significance of energy dissipation. This energy dissipation

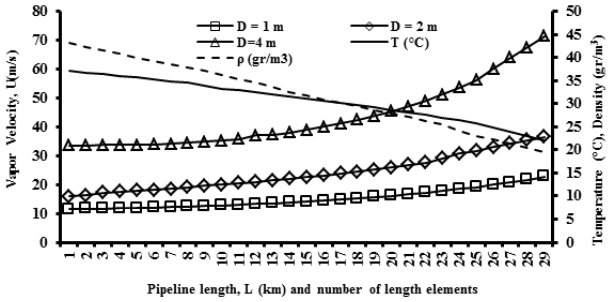

Fig. 6. Elemental partition of the vapor transfer between Bandar Abbas and Geno includes vapor velocity in each element for pipes (diameters of 1, 2, and 4 m) and drop in temperature and density along the path.

is because of friction between fluid and wall that appears greater for smaller diameters. Meanwhile, in the small diameters (0.35 inches), due to the dominance of the incompressible state, a good agreement was reached between the experimental results and the prediction of fluid incompressibility. Other investigators in their lab experiments did not attempt to test the desalination beyond 0.35 inches to determine the effect of the diameter change in vapor transmission.

As observable in Table 3, desalinated water production increases with an increase in the diameter and the production rate is much higher than the pipe diameter variation rate. For a 4 m diameter pipe, a production of 15 kg of desalinated water per second is possible. The computational basis of this research can now be applied to the two cities of Al-Quran and Sana'a (which came from the field studies). This comparison leads to the formation of Tables 4 and 5, which are essentially similar to the structure of Table 3. In Tables 4 and 5, mass numbers calculated from this study are still greater.

Since diameter has an essential influence on water production (m, kg/s), the term "specific desalinated water production (SDWP)" which is directly related to the unit area of the pipe cross-section could be defined. This term can be determined by dividing the water production to the cross-section area. Therefore, the defined have a unit equal to kg/s m^2.

The application of extreme conditions creates complexities, instabilities, and disturbances in computing, which is not within the scope of the objectives and the problem-solving of this paper, and actually disrupts the path to the calculations and the results of this research. Involving the instability problem and introducing the term of extreme changes of time/temperature and extreme changes in velocity can, in practice, be related to extreme weather changes, such as storms, which can be studied in their own right as an independent study.

In a material comparison, it can be easily understood that the mass of materials used in the warm zone and the cold destination are very small compared to the mass that is considered for the SAVP transmission (pipeline). From an engineering point of view, this fact draws on the importance of capital investment for pipelines and it is likely that in terms of project management, significant attention will be devoted to this phase. Despite the fact that beyond the length of the vapor transmission line, presently, the industry producing high-quality and light pipes in various diameters with acceptable strength, mass, heat-insulation, ease of installation, and operation skill is at an assuring stage, and due to an investment return in proper time, there seems to be no limitations for piping. Therefore, the SAVP transmission method can be made applicable by performing conventional, environmental, and meteorological studies, with good oversight on the temperature conditions of the origin, destination, and selection of the correct points for transmission.

Another point that has to be considered is that in case the temperature falls below zero in the mountain, the system will clog due to freezing and it will be incapacitated. This limitation has to be considered in selecting the piping location based on the climatological and weather history of the region. In case water provision is necessary for places with

Table 4
Vapor transmission calculations based on SAVP for diameters of 1, 2, and 4 m for Al-Quran along with results of calculations based on Inoue et al. [1]

Month	D = 1 m				D = 2 m				D = 4 m			
	[1] (cal.)	This work (cal.)		This work (cal.)	[1] (cal.)	This work (cal.)		This work (cal.)	[1] (cal.)	This work (cal.)		This work (cal.)
	m (kg/s)	m (kg/s)	Diff. (%)	Re × 10^3	m (kg/s)	m (kg/s)	Diff. (%)	Re × 10^3	m (kg/s)	m (kg/s)	Diff. (%)	Re × 10^3
January	0.121	0.154	21.4	8.791	0.481	0.521	7.7	29.74	2.652	2.955	10.2	168.678
Febuary	0.136	0.175	22.3	9.989	0.412	0.433	4.8	24.717	2.346	2.743	14.4	156.577
March	0.178	0.202	11.9	11.531	0.393	0.411	4.4	23.461	2.234	2.651	15.7	151.325
April	0.196	0.246	20.3	14.042	0.324	0.332	2.4	18.951	1.727	1.843	6.3	105.203
May	0.265	0.371	28.5	21.178	0.261	0.265	1.5	15.127	1.389	1.512	8.1	86.308
June	0.283	0.384	26.3	21.92	0.246	0.247	0.4	14.099	1.343	1.588	15.4	90.647
July	0.365	0.414	11.8	23.632	0.252	0.258	2.3	14.727	1.382	1.658	16.6	94.642
August	0.310	0.383	19.1	21.863	0.243	0.246	1.2	14.042	1.445	1.635	11.6	93.33
September	0.264	0.316	16.4	18.038	0.265	0.272	2.6	15.526	1.765	2.141	17.5	122.213
October	0.292	0.342	14.6	19.522	0.471	0.541	12.9	30.882	2.747	3.158	13.1	180.266
November	0.209	0.271	22.9	15.469	0.432	0.453	4.6	25.858	2.324	2.712	14.3	154.807
December	0.179	0.232	22.8	13.243	0.594	0.651	8.7	37.161	3.334	3.845	13.2	219.481

Diff. means difference between two formulations and “cal.” stands for “calculated”.

Table 5
Vapor transmission calculations based on SAVP for diameters of 1, 2 and 4 m for Sana'a along with results of calculations based on [1]

Month	D = 1 m				D = 2 m				D = 4 m			
	[1] (cal.)	This work (cal.)		This work (cal.)	[1] (cal.)	This work (cal.)		This work (cal.)	[1] (cal.)	This work (cal.)		This work (cal.)
	m (kg/s)	m (kg/s)	Diff. (%)	Re × 10^3	m (kg/s)	m (kg/s)	Diff. (%)	Re × 10^3	m (kg/s)	m (kg/s)	Diff. (%)	Re × 10^3
January	0.101	0.132	23.5	9.35	0.412	0.433	4.9	24.717	2.667	3.055	12.7	174.386
Febuary	0.115	0.145	20.7	10.277	0.354	0.361	1.9	20.607	2.142	2.484	13.8	141.792
March	0.163	0.184	11.4	11.503	0.367	0.376	2.4	21.463	2.245	2.632	14.7	150.241
April	0.183	0.227	19.4	12.958	0.381	0.393	3.1	22.433	2.361	2.756	14.3	157.319
May	0.242	0.351	31.1	20.036	0.393	0.464	15.3	26.486	2.431	2.841	14.4	162.171
June	0.263	0.376	30.1	21.463	0.426	0.442	3.6	25.23	2.658	3.147	15.5	179.638
July	0.334	0.401	16.7	22.89	0.485	0.533	9.1	30.425	2.753	3.398	18.9	193.966
August	0.305	0.374	18.4	21.349	0.481	0.539	10.7	30.767	2.752	3.315	16.9	189.228
September	0.247	0.304	18.7	17.353	0.625	0.675	7.4	38.531	3.575	4.153	13.9	237.063
October	0.282	0.331	14.8	18.894	0.566	0.591	4.2	33.736	3.324	3.884	14.4	221.708
November	0.201	0.244	17.6	13.928	0.578	0.583	0.8	33.279	2.851	3.352	14.9	191.34
December	0.183	0.219	16.4	12.501	0.451	0.465	3.1	26.543	2.625	3.087	15.1	176.213

Diff. means difference between two formulations and "cal." stands for "calculated".

the possibility of the temperature dropping below zero at the destination, L_C can be determined through calculations and fluid discharge and collection equipment, such as a pressure or vacuum-maintaining valve, and a reservoir.

7. Conclusion

Desalination of seawater could be down by a potential of the natural temperature difference between a warm source (seawater) and cold source (a hill or short maintains) through the natural movement of water vapor from sea level and its condensation at the hill. This technique is called the SAVP in which no external energy (except initial energy for pipeline vacuum for the first time, once only for commissioning) is needed for desalination. In accordance with some restricted lab observations and mass calculations, other studies already have concluded that vapor transmission could be generally produces desalinated water. However, the effects of many facts and factors such as: applying of SAVP in a more real scale device for desalination along with real potential of temperature differences and reliable pipeline diameters, the effect of salt concentrations, and fluid compressibility (and more) have been missed or neglected experimentally and theoretically. We purely concluded that SAVP could be applied not only in lab-scaled devices but also in huge inlands or open areas. This conclusion performed by preparing of complimentary and reliable experimental data as well as strong theories consists of vapor momentum, friction, fluid thermodynamics (osmotic coefficient for salinity and equilibrium), mass, and energy equations. Temperature difference, salinity, and pipeline diameters are three main factors that their effects were analyzed theoretically and technically for SAVP. Physically and in accordance to the current principles in the transport phenomena, by considering the technology and the ability of mankind in the construction of long pipelines, the SAVP is both practical and logical. There are many benefits (such as extreme energy reduction or its elimination, elimination of evaporating and condensing devices, extreme reduction in energy consumption or its elimination related to the water transfer, the possibility of regaining energy at the transfer destination by using a water turbine, water distribution by gravity, and the use of advantages allocated by the Paris Convention, February 2006) to the production of desalinated water through this transfer, which has attracted the attention of researchers in the development of this method. Transitional cross-section area, excessive temperature

Nomenclature

Symbols	Parameters	Range	Unit
a_W	Water activity coefficient	Up to 1	DL*
D	Diameter of pipe	1–4	m (land)
		0.35–1	inch (lab)
f	Fanning friction factor	0–0.1	DL
g	Acceleration due to gravity	9.81	m/s^2
H	Difference in elevation	Up to 2,300	m (land)
		Up to 11	m (lab)
L	Length of transport part	30–160	km (land)
		Up to 180	m (lab)
L_C	Length of condensation part	Up to 10	km (land)
m	Production rate of distilled water	Up to 15	kg/s (land)
		Up to 191	g/h (lab)
mo	Molality of NaCl	Up to 6	mol/kg water
P	Pressure or pressure drop	Up to 101	kPa
Re	Reynolds number (vapor)	Up to 862×10^3	DL (land)
		Up to 291	DL (lab)
t	Time	7 to 283	min (land)
		60 to 300	min (lab)
U	Vapor velocity	9–71	m/s (land)
		Up to 16	m/s (lab)
$\gamma^{\pm}$	Mean ionic activity coefficient	Up to 1	DL
ϵ	Pipe roughness	0, smooth pipes	DL (land)
		10^{-6}–10^{-2}	DL (lab)
μ	Water viscosity (liquid)	$(0.798–1.519) \times 10^{-3}$	Pa.s
	Water viscosity (vapor)	$(0.934–1.001) \times 10^{-5}$	Pa.s
ρ	Water density (liquid)	996–1,000	kg/m^3
	Water density (vapor)	Up to 0.03	kg/m^3
Φ	Osmotic coefficient	Up to 1	DL

*DL: dimensionless; underlined numbers are related to referenced research works.

difference, and salinity are effective factors in transporting SAVP. Increasing the diameter as far as possible, choosing the climatic regions that provide maximum natural temperature difference at a minimum distance, and the raw-water options with salinity values less than seawater (such as in effluents and low salinity brackish water) can improve the SAVP efficiency. The calculations of vapor transport without simplifying assumptions, and without interfering assumptions and presumptions about the condensation part, and the consideration of the maximum salinity and the fact that the fluid is compressible provides increasingly more reliable numbers for vapor transfer relative to the modeling of previous researchers.

Acknowledgments

We gratefully acknowledge the help and assistance of Mr. Koosha Aghazadeh, for his cooperation in math and computer programming. Koosha is a graduate student from the School of Civil Engineering, University of Tehran, Iran.

References

[1] K. Inoue, Y. Abe, M. Murakami, T. Mori, Feasibility study of desalination technology utilizing the temperature difference between seawater and inland atmosphere, Desalination, 197 (2006) 137–153.
[2] A. Del Amo, P. Antonio, System and Method for Desalinating Seawater, Patent WO/171986 A1, 2012.
[3] S. Eggleston, L. Buendia, K. Miwa, T. Ngara, K. Tanabe, IPCC Guidelines for National Greenhouse Gas Inventories, Intergovernmental Panel on Climate Change, Paris Convention February, 2006.
[4] L.M. Camacho, L. Dumée, J. Zhang, J. Li, M. Duke, J. Gomez, S. Gray, Advances in membrane distillation for water desalination and purification applications, Water, 5 (2013) 94–196.
[5] L. Awerbuch, Geothermal Desalination Potential for Clean and Affordable New Water Solutions, International Desalination Association (IDA Conference), Miami, 2016.
[6] A.D. Khawaji, I.K. Kutubkhanah, J.M. Wie, Advances in seawater desalination technologies, Desalination, 221 (2008) 47–69.
[7] I.S. Al-Mutaz, I. Wazeer, Current status and future directions of MED-TVC desalination technology, Desal. Water Treat., 55 (2014) 1–9.
[8] A.H.M. Saadat, M.S. Islam, F. Parvin, A. Sultana, Desalination technologies for developing countries: a review, J. Sci. Res., 10 (2018) 77–97.
[9] K. Zotalis, E.G. Dialynas, N. Mamassis, A.N. Angelakis, Desalination technologies: hellenic experience, Water, 6 (2014) 1134–1150.
[10] N. El-Haddad, H. Yared, R. Carbonell, Energy Efficient Desalination: Meeting the GCC's Water Needs in an Environmentally Sustainable Way, International Water Summit (IWS), Environment Agency Abu Dhabi, Sourced and Reported #4, 2018.
[11] S.E. Aly, Energy saving in desalination plants by using vapor thermo-compression, Desalination, 49 (1984) 37–56.
[12] R. Matz, Z. Zimerman, Low-temperature vapor compression and multi-effect desalination of seawater. Effects of design on operation and economic, Desalination, 52 (1985) 201–216.
[13] M. Abdel-Jawad, Energy Sources for Coupling with Desalination Plants in the GCC countries, Consultancy Report Prepared for ESCWA, September, 2001.
[14] T. Szacsvay, M. Posnansky, Distillation desalination systems powered by waste heat from combined cycle power generation units, Desalination, 136 (200) 133–140.
[15] A.E. Muthunayagam, K. Ramamurthi, J.R. Paden, Low temperature flash vaporization for desalination, Desalination, 180 (2005) 25–32.
[16] T. Younos, K.E. Tulou, Overview of desalination techniques, J. Contemp. Water Res. Edu., 132 (2005) 3–10.
[17] B.A. Moore, E. Martinson, D. Raviv, Waste to water: a low energy water distillation method, Desalination, 220 (2008) 502–505.
[18] C.A. Kemper, G.F. Waltham, G.F. Harper, G.A. Brown, Multiple-Phase Ejector Desalination Apparatus and Desalination Process, Patent US/3288685, 1966.
[19] Z.R. Kanaan, M. Ann Arbor, Spray-Type Desalination Using Gas Turbine Exhaust Desalination Heating, Patent US/3425914, 1969.
[20] M.F. Anderson, Sub-Atmospheric Pressure Desalination and/or Cooling Method and Means, Patent US/4366030, 1982.
[21] M.R. Levine, B. Raton, Low Energy Vacuum Desalination Method and Apparatus, Patent US/7431806 B2, 2005.
[22] E. Brauns, Combination of a Desalination Plant and a Salinity Gradient Power Reverse Electro-Dialysis Plant and Use Thereof, Patent EP/1746680 A1, 2007.
[23] E. Brauns, Combination of a Desalination Plant and a Salinity Gradient Power Reverse Electro-Dialysis Plant and Use Thereof, Patent US/0230376 A1, 2008.
[24] S. Shelley, Pipeline System, Patent US/0044206 A1, 2010.
[25] A.D. Akers, Tower for the Desalination of Seawater, Patent US/7897019 B2, 2011.
[26] B.E. Nadeau, K.P. Rock, Desalination Apparatus, Patent US/0133356 A1, 2013.
[27] J. Wellmann, K. Neuhäuser, F. Behrendt, M. Lehmann, Modeling an innovative low-temperature desalination system with integrated cogeneration in a concentrating solar power plant, Desal. Water Treat., 55 (2015) 3163–3171.
[28] J. Wellmann, T. Morosuk, Renewable energy supply and demand for the city of El-Gouna, Egypt, Sustainability, 314 (2016) 1–27.
[29] J.F. Branco, C. Pinho, R.A. Figueiredo, From a Power-Law Equation for the Friction Factor in Smooth Pipes to a Controversy on the Overlap Layer, The 6th International Conference on Energy and Environment Research, Portugal, 2001.
[30] T. Maruzen, Fundamentals of Fluids Mechanics (The Japan Society of Mechanical Engineers, JSME), A Mechanical Engineers' Handbook, Tokyo, 1986.
[31] M.H. Sharqawy, J.H. Lienhard, S.M. Zubair, Thermo-physical properties of seawater: a review of existing correlations and data, Desal. Water Treat., 16 (2010) 354–380.
[32] K.S. Pitzer, Chapter 6: Activity Coefficients in Electrolyte Solutions, 2nd ed., CRC Press, London, 1991.
[33] Meteorological Organization Country. Available at: http://www.irimo.ir